Volume 23
Number 5
7 February 2025
Pages 969-1222

Organic & Biomolecular Chemistry

rsc.li/obc

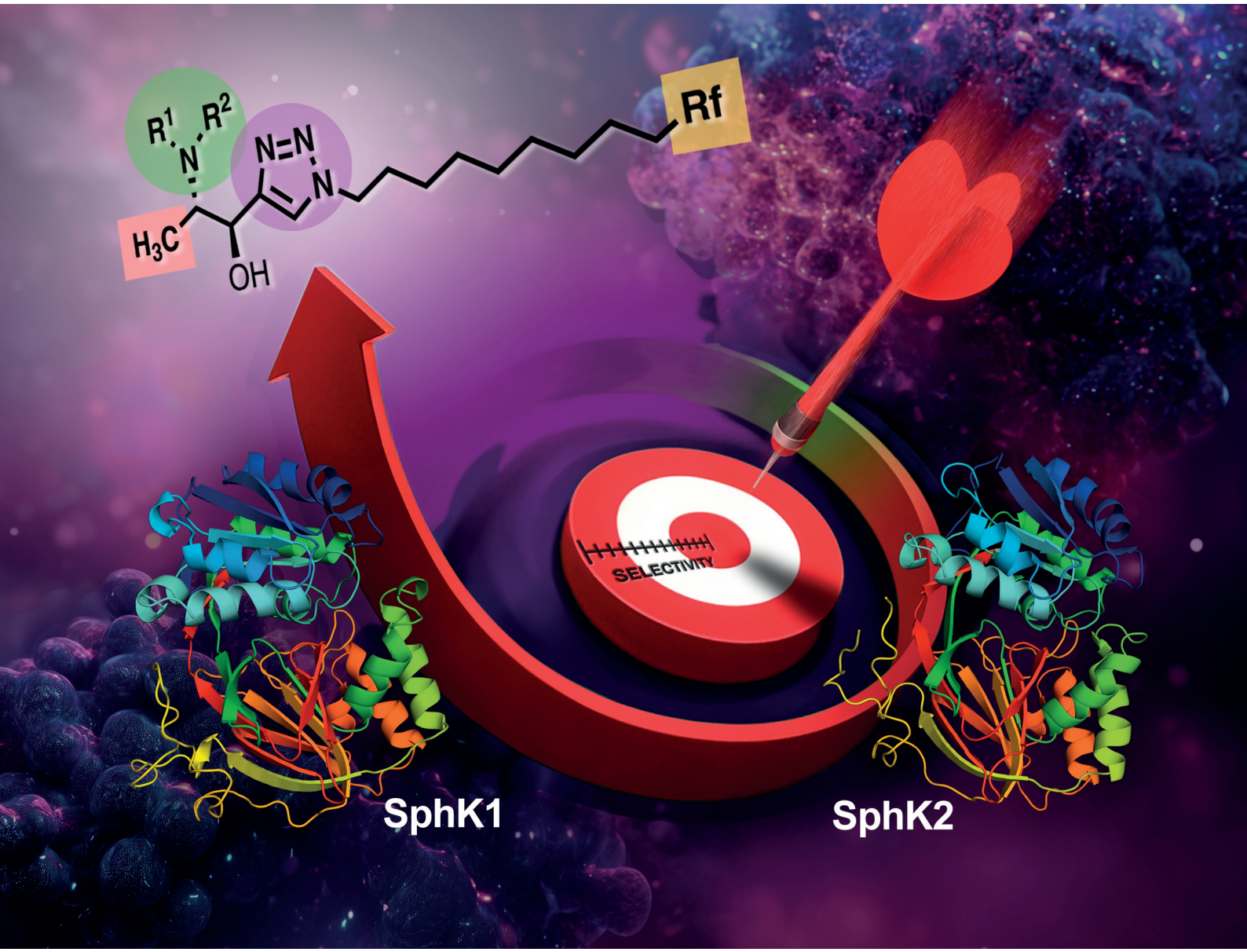

ISSN 1477-0520

ROYAL SOCIETY OF CHEMISTRY

PAPER
Yolanda Díaz, M. Isabel Matheu *et al.*
Syntheses of differentially fluorinated triazole-based 1-deoxysphingosine analogues *en route* to SphK inhibitors

Organic & Biomolecular Chemistry

ROYAL SOCIETY OF CHEMISTRY

PAPER

View Article Online
View Journal | View Issue

Cite this: *Org. Biomol. Chem.*, 2025, **23**, 1104

Syntheses of differentially fluorinated triazole-based 1-deoxysphingosine analogues *en route* to SphK inhibitors†

Adrià Cardona, ‡[a] Varbina Ivanova, ‡[b] Raúl Beltrán-Debón, [c] Xavier Barril, [b] Sergio Castillón, [a] Yolanda Díaz *[a] and M. Isabel Matheu *[a]

This study focuses on the stereoselective syntheses of 1-deoxysphingosine analogues as potential inhibitors of sphingosine kinase (SphK), particularly targeting its isoforms SphK1 and SphK2, which are implicated in cancer progression and therapy resistance. The research builds on previous work by designing a series of analogues featuring systematic structural modifications like the incorporation of a triazole ring, varying degrees of fluorination, and different head groups (*e.g.*, guanidino, *N*-methylamino, and *N*,*N*-dimethylamino). These modifications aimed to enhance polar and hydrophobic interactions especially with SphK2. The synthesized compounds were evaluated for their inhibitory activity, revealing that certain derivatives, particularly those with guanidino groups and heptafluoropropyl fragments at the lipidic tail, exhibited significant potency and selectivity towards SphK2. Docking studies supported these findings by showing favorable binding interactions within the SphK2 active site, which were less pronounced in SphK1, correlating with the observed selectivity. This work contributes to the development of novel 1-deoxysphingosine analogues targeting SphK inhibition, as well as to the knowledge of the differential topology of the active sites in SphK1 and SphK2.

Received 14th October 2024,
Accepted 8th November 2024

DOI: 10.1039/d4ob01656d

rsc.li/obc

Introduction

Sphingosine kinase (SphK) plays a pivotal role in regulating the sphingolipid rheostat[1] (Scheme 1), which governs the dynamic balance between ceramide (Cer) and sphingosine 1-phosphate (S1P). Depending on the position of this rheostat, programmed cell death (Scheme 1, top) or cell survival (Scheme 1, bottom) is promoted,[2] since Cer and sphingosine (Sph) induce cell apoptosis and growth arrest, whereas S1P promotes cell survival and proliferation.

In this equilibrium, SphK catalyzes the ATP-dependent phosphorylation of sphingosine (Sph) to produce sphingosine 1-phosphate (S1P). This enzyme exists in two isoforms, SphK1 and SphK2,[3] which differ in their substrate preference, subcellular localizations and tissue distributions.[4]

The focus on SphK inhibitors as potential drugs arises from the observation that SphK1 is often overexpressed in a wide range of tumors, including solid tumours[5] and leukaemia.[6] Hence, SphK inhibition is associated with tumor cell apoptosis. Moreover, SphK1 is involved in induction of chemotherapeutic resistance[5b] and radiotherapy-resistant tumour cells or those with acquired chemoresistance exhibit elevated expression of SphK1.[7] Besides, the potential of SphK2 as a

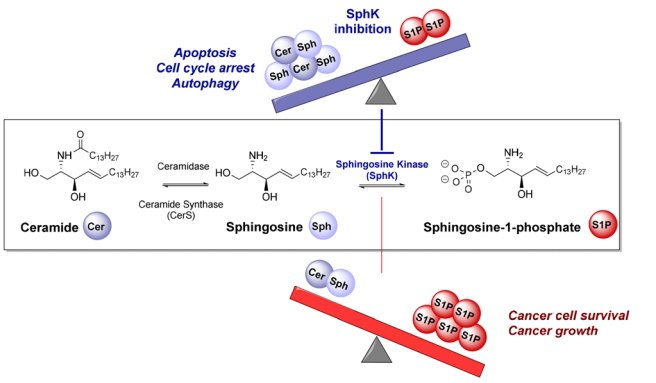

Scheme 1 Sphingolipid rheostat and SphK inhibition effects.

[a]*Universitat Rovira i Virgili, Departament de Química Analítica i Química Orgànica, Faculty of Chemistry, C/Marcel·lí Domingo 1, 43007 Tarragona, Spain. E-mail: maribel.matheu@urv.cat*
[b]*Universitat de Barcelona, Department of Physical Chemistry, Faculty of Pharmacy, Av. Joan XXIII s/n, Barcelona 08028, Spain*
[c]*Universitat Rovira i Virgili, Departament de Bioquímica i Biotecnologia, Faculty of Chemistry, C/Marcel·lí Domingo 1, 43007 Tarragona, Spain*

†Electronic supplementary information (ESI) available: Experimental details, NMR spectra, additional docking figures and inhibition curves. See DOI: https://doi.org/10.1039/d4ob01656d

‡These authors contributed equally.

target for tumor cells has emerged more recently.[8] Thus, significant efforts have been made looking for effective sphingosine kinase inhibitors.[9]

Interest in 1-deoxysphingolipids has grown due to their remarkable biological properties, including antiproliferative and cytotoxic activities, as well as their influence on sphingolipid biosynthesis and metabolism.[10] Thus, the isolation of the first antiproliferative 1-deoxysphingolipid, spisulosine,[11] and its close structural relationship with other related 1-deoxysphingoid bases with remarkable cytotoxic properties, such as clavaminols,[12] crucigasterins,[13] xestoaminols[14] or enigmol[15] (Fig. 1), make this class of compounds an attractive lead for anticancer-oriented drug discovery.

The rationale for designing 1-deoxy analogues is to mimic the antiproliferative cytotoxic effects of sphingosine, while preventing the phosphorylation of the primary alcohol group that leads to unwanted mitogenic and anti-apoptotic activities. In this sense, one representative compound is enigmol (Fig. 1), distinguished from other 1-deoxysphingolipids by an additional hydroxyl group at the C-5 position, which imparts to this compound a polarity similar to that of sphingosine. Biological studies have shown that enigmol inhibits sphingosine kinase,[15] ceramide synthase[16] and protein kinase,[17] exhibiting a broad spectrum of cytotoxicity ($0.4\ \mu M \leq IC_{50} \leq 14\ \mu M$) against 57 human cancer cell lines including colon, breast, brain and prostate.[15] Additionally, enigmol's modest *in vitro* potency is compensated by its favourable pharmacokinetic properties *in vivo*.[15]

During the past years, we have been involved in developing methods for the synthesis of sphingoid bases,[18] intended to be efficient sphingolipid-derived SphK inhibitors.[19] In this context, we had explored the synthesis of sphingosine analogues incorporating a rigid triazole moiety in the aliphatic chain mimicking the conformational restriction provided by the 4,5-double bond in sphingosine.§ These analogues featured systematic modifications in the polar head and varying degrees of fluorination at the terminus of the aliphatic chain (Fig. 1, X = CH_2OH).[19a] Compounds with a heptafluoro tail (Fig. 1) displayed the highest inhibitory activity against SphK2 in the low micromolar range while presenting the highest SphK2/SphK1 selectivity.

Reasons for introducing these structural modifications (Fig. 1) were: (a) the heterocyclic scaffold should be capable of establishing additional interactions with residues in the throat of the binding site of the enzyme and display a strong dipole moment;[20] (b) derivatization of the free amino group into *N*,*N*-dimethylamino, guanidino, and *N*-methylamino moieties is expected to enhance polar interactions at the enzyme's binding site while likely preventing the acylation of the *N*-moiety, thereby slowing down enzymatic diversion to other sphingolipids,[15] and (c) modification of the lipophilic end *via* a gradual increase in the degree of fluorination with perfluorinated terminal fragments to exploit interactions[21] of the fatty tail of the sphingolipid with the hydrophobic bottom of the SphK binding site.[22] Additionally, fluorine's stereoelectronic effects can influence the conformation of the flexible alkyl chain. Thus, strategically incorporating perfluorinated lipid fragments and finding the appropriate degree of fluorination may enhance affinity for the SphK binding site through entropy gain.[23]

In this context, we present here the syntheses and SphK1/SphK2 inhibitory effect of 1-deoxysphingosine analogues (Fig. 1, X = CH_3) in which the above-mentioned modifications —1,2,3-triazole unit, derivatization of the amino group, and fluorination of the lipophilic tail—introduced in our previous work are explored.

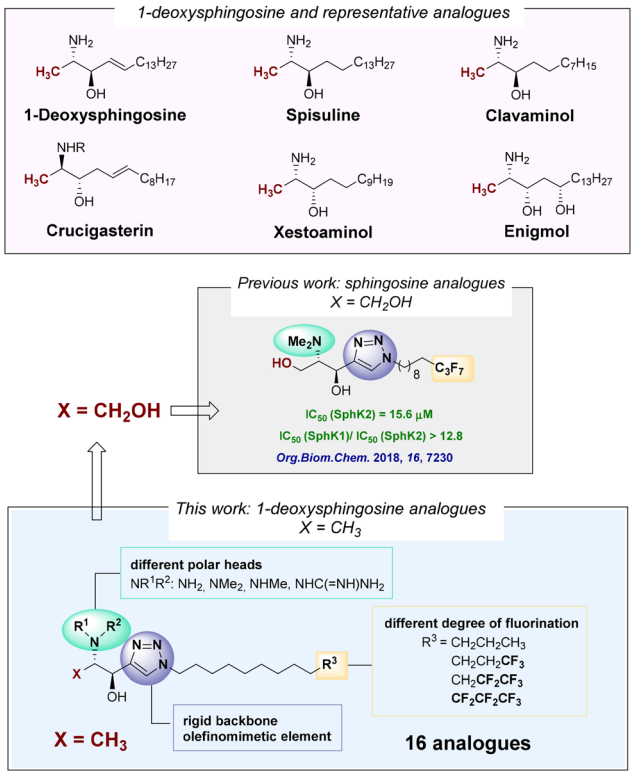

Fig. 1 Representative compounds, previous work on sphingosine analogues, and structural modifications proposed in this work.

Results and discussion

The synthesis of target compounds **1–4a–d** (Scheme 2) was envisaged through a diastereoselective synthesis starting from commercially available L-alaninol. The construction of the *anti*-2,3-aminoalcohol segment present in 1-deoxysphingosine was envisioned *via* diastereoselective nucleophilic addition of an organoalkynylide species to L-alaninal, by the use of appropriate protecting groups on the amino group. Addition of Grignard reagents to chiral *N*-disubstituted amino aldehydes with bulky substituents such as benzyl moieties usually pro-

§ Relevant studies on this topic can be found in ref. 9*b–d*.

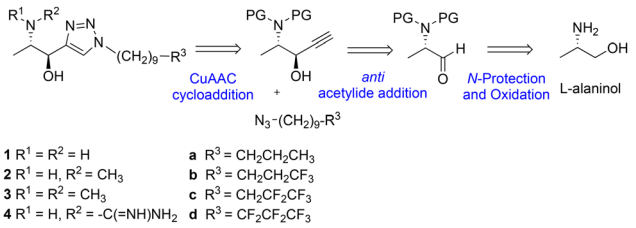

Scheme 2 Retrosynthetic pathway of triazole-based 1-deoxysphingolipid analogues.

ceeds under Felkin conditions to afford 1,2-amino alcohols in excellent *anti* diastereomeric ratios.[24] Thus, the syntheses of the corresponding *N*,*N*-dibenzyl *anti*-2-amino-3-alcohols **8** started with the protection of the amino group at L-alaninol, subsequent Swern oxidation and *in situ* addition of the acetylide Grignard reagent to the protected α-amino aldehyde intermediate (based on a one-pot methodology by Silveira-Dorta *et al.*)[25] (Scheme 3). For the sake of comparison, the analogous processes using phthalimido and NHBoc functionalities in alcohols **6** and **7** were also explored. As expected, one-pot oxidation/addition of ethynyl magnesium bromide starting from dibenzylamino derivative **5** proceeded with high selectivity to form *anti*-configured alcohol **8**. In contrast, the reaction of phthalimido derivative **6** led to the formation of the amino alcohol **9** with null stereoselectivity, whereas the monoprotected Boc derivative **7** led to the preferential formation of the *syn*-diastereoisomer **10** (Scheme 3).

Syntheses of the alkyltriazole derivatives

Propargyl alcohol **8** was then selected for following the synthetic scheme. The reaction of dodecyl azide (**11a**)[19a] with **8** under typical conditions for copper-catalysed azide–alkyne cycloaddition (CuAAC) ($CuSO_4{\cdot}5H_2O$ and sodium ascorbate) in DMSO : H_2O as a solvent at 65 °C furnished triazole **12a** in a 43% yield as a single diastereomer after purification of the diastereomeric mixture obtained. A 55% yield of diastereomerically pure **12a** was obtained using a CH_2Cl_2/H_2O mixture at room temperature (Scheme 4). Debenzylation with H_2 and Pd/C in methanol afforded amine **1a** in 88% yield.

The preparation of the *N*-methyl derivative **2a** was assayed from **1a** *via* reductive amination with aqueous formaldehyde under various reactions conditions such as $NaBH_3CN$ in MeOH, or zinc under neutral conditions (NaH_2PO_4);[26]

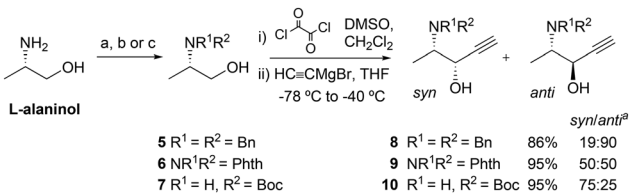

Scheme 3 Syntheses of amino-alcohol intermediates **8–10**. For **5**: (a) BnBr, K_2CO_3, H_2O/acetone (1 : 1); for **6**: (b) phthalic anhydride, PhMe; for **7**: (c) Boc_2O, Et_3N, THF. [a] Determined by NMR.

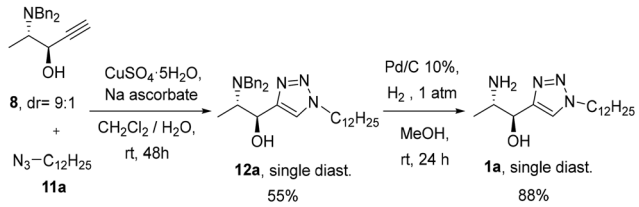

Scheme 4 Preparation of **1a** *via* CuAAC reaction and deprotection.

however, a mixture of the starting amine and dimethyl- and monomethyl amino derivatives was obtained. The best conditions were found by reduction of the *N*-Boc protected compound **13a** with $LiAlH_4$ to render compound **2a** in 61% yield over the two steps (Scheme 5). Additionally, compound **1a** was also reacted with *p*-formaldehyde under reductive conditions to afford *N*,*N*-dimethyl amino compound **3a** in 76% yield.

Parallelly, treatment of **1a** with *N*,*N*′-di-Boc-1*H*-pyrazole-1-carboxiamidine (**14**) in the presence of triethylamine followed by reaction with TFA in CH_2Cl_2 rendered a guanidine derivative as a zwitterionic trifluoroacetate species, which by washings with aqueous NaOH gave free guanidine derivative **4a** (Scheme 5).

Syntheses of partially fluorinated triazole sphingolipid analogues

Propargyl alcohol **8** was subjected to CuAAC with partially fluorinated azides **11b**, **11c** and **11d**,[19a] followed by concomitant amino deprotection and hydrogenation of the alkene moiety in **12b–d** to render sphingolipid analogues **1b–d**, respectively, in good yields (Scheme 6).

In line with the derivatization of the parent non-fluorinated sphingolipid **1a**, fluorinated compounds **1b–d** were converted into the *N*-methyl, *N*,*N*-dimethyl and guanidinium trifluoroacetates derivatives **2b–d**, **3b–d** and **4b–d**, respectively (Scheme 7).

In vitro sphingosine kinase assays

In vitro inhibition potency in front of SphK of compounds **1a–d**, **2a–d**, **3a–d**, **4a–d** was measured *via* time-resolved fluo-

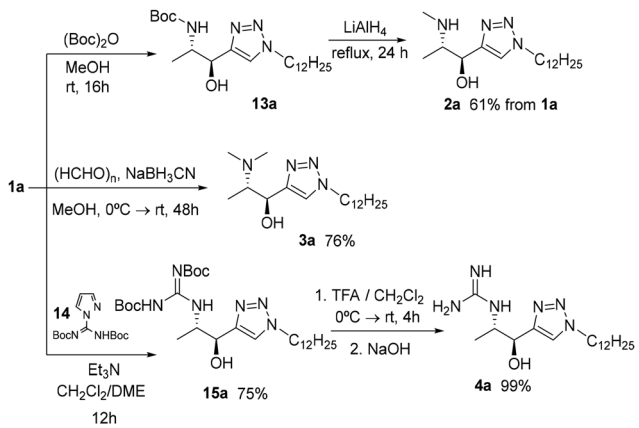

Scheme 5 Derivatisation of the amino moiety in **1a** to give 1-deoxysphingolipid analogues **2a**, **3a** and **4a**.

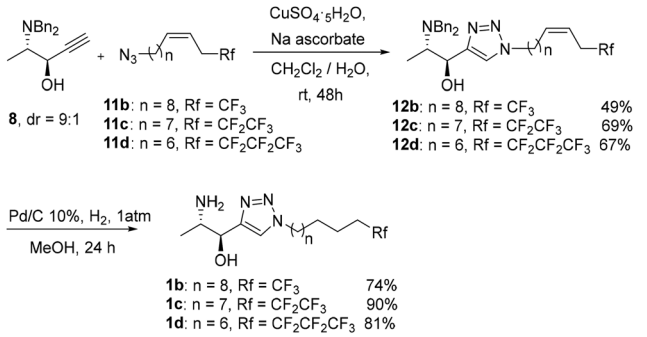

Scheme 6 Syntheses of fluorinated 1-deoxysphingolipids **1b–d**.

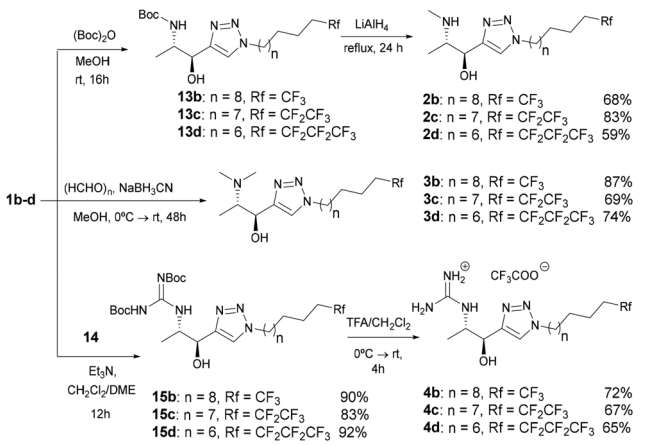

Scheme 7 Derivatisation of the amino moiety in **1b–d** to give fluorinated 1-deoxysphingolipid analogues **2b–d**, **3b–d** and **4b–d**.

Table 1 IC_{50} values of compounds **1a–d**, **2a–d**, **3a–d**, **4a–d** and the reference (DMS) for SphK1 and SphK2 inhibition

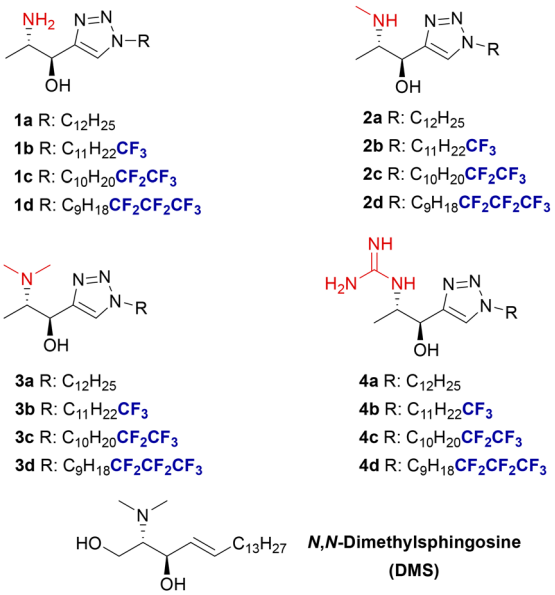

Inh.	IC_{50}[a] SphK1	IC_{50}[a] SphK2	Sel.[b]	Inh.	IC_{50}[a] SphK1	IC_{50}[a] SphK2	Sel.[b]
1a	34.8	18.9	1.8	**3a**	92.3	10.0	9.2
1b	127.0	57.4	2.2	**3b**	112.0	57.3	2.0
1c	118.0	>200	<0.6	**3c**	>200	39.4	>5.0
1d	71.3	18.8	3.8	**3d**	>200	>200	—
2a	86.9	20.8	4.2	**4a**	50.1	5.0	10.0
2b	>200	47.2	2.5	**4b**	77.6	29.2	2.7
2c	95.3	23.6	4.0	**4c**	51.4	9.0	5.7
2d	62.1	25.4	2.4	**4d**	19.9	6.4	3.1
DMS	27.7	1.4	19.8				

[a] Values are expressed as concentrations (μM). [b] Sel. refers to the SphK2/SphK1 selectivity ratio (IC_{50}Sphk1/IC_{50}Sphk2).

rescence resonance energy transfer (TR-FRET) analysis that relies on the immunodetection of adenosine diphosphate (ADP).[27,28] The half maximal inhibitory concentrations of the synthesized 1-deoxysphingosine analogues were determined independently for SphK1 and SphK2 using dimethyl sphingosine (DMS) as a reference (Table 1).

The 1-deoxysphingolipid derivatives synthesized acted as dual inhibitors against SphK1 and Sphk2, with activities in the micromolar range (Table 1), comparable to those of the sphingosine derivatives previously synthesized in our group.[19a] As a general trend, compounds **1a–d**, **2a–d**, **3a–d**, and **4a–d** demonstrated greater activity against SphK2 compared to SphK1, with selectivity ratios reaching up to 10 for the non-fluorinated dimethyl and guanidinium derivatives **3a** and **4a** respectively. However, this selectivity did not surpass that of the reference dual inhibitor DMS. The selectivity for sphingosine kinase 2 (IC_{50}SphK1/IC_{50}Sphk2) does not show a consistent correlation with the degree of fluorination in the lipophilic tail across the series of compounds, highlighting the complex nature of interactions within the SphK binding sites.

The least active derivatives for each series towards both SphK isoforms were invariably those with the terminal trifluoromethyl residues (**1b**, **2b**, **3b** and **4b**). In some cases, the pentafluoroethyl or heptafluoropropyl fragment also had a negative impact on the inhibitory activity (**1c**, **3c**, **3d**).

For each headgroup, the most active derivatives towards SphK2 were the native non-fluorinated sphingolipids (**a**, IC_{50} = 5.0–20.8 μM) and in most of the cases the heptafluorinated derivatives (**1d**, IC_{50} = 18.8 μM; **2d**, IC_{50} = 25.4 μM; **4d**, IC_{50} = 6.4 μM). Within the same degree of fluorination, the inhibitory activity was not very sensitive to the nature of the polar headgroup, and especially against SphK2.

The most active sphingolipid inhibitor against SphK2 was the guanidino derivative **4a** (IC_{50} = 5.0 μM, SphK2/SphK1 selectivity ratio of 10.0), followed by heptafluoro and pentafluoro guanidino derivatives **4d** (IC_{50} = 6.4 μM) and **4c** (IC_{50} = 9.0 μM), and by the non-fluorinated dimethylamino derivative **3a** (IC_{50} = 10.0 μM, SphK2/SphK1 selectivity ratio of 9.2).

The inhibitory activity against SphK1 was, as mentioned above, comparatively lower, and in parallel to the results against SphK2, the best inhibitor is among the guanidino series (**4d**, IC_{50} = 19.9 μM), followed by the non-fluorinated free-amino derivative **1a** (IC_{50} = 34.8 μM).

In summary, the compounds that showed the best inhibitory activity against SphK2 ($IC_{50} \leq 10$ μM) were **3a**, **4a**, **4c**, and **4d**. Regarding SphK2/SphK1 selectivity, the highest selectivity was observed for **4a** (10.0) and **3a** (9.2). For SphK1 inhibitory activity, the most active compounds ($IC_{50} < 35$ μM) were **4d** and **1a**.

Docking studies

To better understand the data obtained from the inhibitory activity assays, the potential binding modes of a selected group of synthesized compounds were evaluated by employing a combination of homology modelling and molecular docking. Specifically, we focused on the best SphK2 inhibitors among the products synthesized, the *N*,*N*-dimethyl analogue **3a** and guanidino derivatives **4a**, **4c**, and **4d** (**3a** and **4a** are also the most selective), and **3b** and **4b**, for comparative purposes.

Ligand flexibility is a key factor in molecular docking, as increased degrees of freedom may compromise exhaustive sampling. For very flexible ligands (more than 20 rotatable bonds), it is necessary to increase sampling parameters.[29] In this study, the compounds have moderate flexibility, with up to 15 rotatable bonds and we could observe convergence. However, protein flexibility is not considered, and therefore we interpret binding poses and docking scores with caution. Additionally, as polar interactions drive selective molecular recognition, we focused our analysis on the interactions formed by the polar heads, while the flexible aliphatic tails of the compounds were included in the docking studies to better match the binding pocket's size and shape.

Most amino acids in the binding sites of SphK1 and SphK2 are conserved,[19b,30] except for key differences at the throat and toe of the binding channel. In SphK1, Ile174, Met272, and Phe288 are replaced by Val340, Leu553, and Cys569 in SphK2. These substitutions cause structural changes in the binding channel, with bulkier residues in SphK1 narrowing the space, while smaller ones in SphK2 create a wider channel. This also affects the orientation of key residues, such as Arg357 in SphK2, which is more exposed for polar interactions compared to Arg191 in SphK1 at the mouth of the binding site.

Molecular docking of 3a–b and 4a–d against SphK2. The most active compounds, **3a**, **4a**, **4c**, and **4d**, share several key interactions with SphK2 that contribute to their inhibition capacity. One of the best scored poses for **4a** in SphK2 is shown in Fig. 2 as an example (those for compounds **3a**, **4c**, and **4d** can be seen in Fig. 3–5 of the ESI†).

First, as a result of the recontouring of SphK2's throat in relation to that of SphK1,[30] the triazole ring is able to stabilize the binding through π-stacking interactions with Phe358.

The hydroxyl group at position 3 of the ligand is another common feature that consistently forms a hydrogen bond with Asp344 in all the most active compounds. This interaction pattern stabilizes the compounds' binding poses and contributes to their lower IC_{50} values.

Regarding the polar headgroups of these compounds, the *N*,*N*-dimethyl head in **3a** adopts a linear conformation, facilitating the formation of polar OH-3 interactions. For **4a**, **4c** and **4d**, the guanidino group adopts a bent orientation with respect to the main chain and is thus exposed to polar residues in the mouth of the binding site, forming additional hydrogen bonds with Asp247 (*via* a primary amine group) and the backbone carbonyl group of Leu549 (*via* primary and secondary amine groups), further strengthening the interactions and enhancing activity when compared to *N*,*N*-dimethyl amino derivative **3a**.

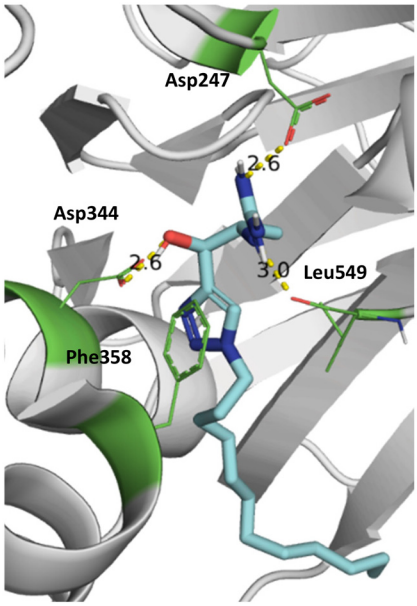

Fig. 2 Example of one of the best scored poses in Sphk2 for compound **4a**.

Finally, the interaction of the hydrophobic tail with the toe of the binding site varies among the compounds. In **3a** and **4a**, the tail adopts a J-shaped orientation that fits well into the hydrophobic pocket. For **4c** and **4d**, the presence of polyfluorinated fragments in the tail provides additional rigidity, enhancing the fit within the channels.

The best-scoring docking poses of the less active compounds **3b** and **4b** (Fig. 6 in the ESI†) reveal a flipped orientation of the heteroaromatic ring, potentially disrupting π-stacking interactions with Phe358 and resulting in a suboptimal alignment of the hydroxyl hydrogen, which hinders hydrogen bond formation with Asp344. No docking poses were observed with the optimal alignment of this hydrogen atom, which likely contributes to their reduced activity.

It is noteworthy that for compound **3b**, some of the best scored poses have the fluorinated tail in the polar part of the pocket.¶ This could explain the unvaryingly higher IC_{50} value

¶Although the bulkier nature of the terminal trifluoromethyl group compared to a methyl group could favour *a priori* a better accommodation of the end of the hydrophobic chain in the toe of the J-shaped channel of the enzyme (more expanded for SphK2 than for SphK1),[30] the higher polarity of this group could promote interactions with the polar residues at the head of the active site, preventing the compound from entering the J-shaped channel.

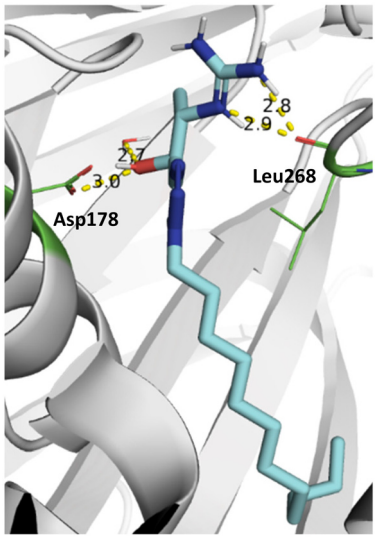

Fig. 3 Example of one of the best scored poses in Sphk1 for compound **4a**.

of the trifluoromethyl derivatives in the different series of compounds.

Molecular docking of 3a–b and 4a–d against SphK1. The molecular docking analysis of the most active compounds—**3a**, **4a**, **4c**, and **4d**—highlights some interactions with SphK1 that could drive their higher binding efficiencies (one of the best scored poses for **4a** in SphK1 is shown in Fig. 3 as an example, while those for compounds **3a**, **4c**, and **4d** can be seen in Fig. 7–9 of the ESI†).

With respect to the heterocyclic moiety, in compounds **3a** and **4a**, the triazole ring occupies a higher position, closer to the polar head, within the binding cavity of SphK1 compared to SphK2, moving closer to Asp178. This is due to structural differences among the two isoforms (available surface area and shape) in the binding pocket as a result of the presence of Ile174 and Met272 in SphK1, compared to Val340 and Leu553 in SphK2. This altered positioning of the ligands in the throat of the protein channel diminishes interactions with Phe192, which withdraws from the cavity with respect to Phe358 in SphK2, reducing the binding strength compared to that seen in the SphK2 isoform. As the triazole moiety is not anchored by Phe192 in Sphk1, the compounds are more flexible in the kinase binding site and can adopt different binding modes. For **3a**, an additional hydrogen bond interaction involving one triazole nitrogen and a structural water molecule is observed (Fig. 7, ESI†). In the trifluoromethylated compound **3b**, however, the orientation of the triazole group shifts, leading to a suboptimal alignment of the hydroxyl hydrogen compared to that observed in **3a**. For compounds **4c** and **4d**, the triazole ring shifts higher within the pocket, although it still plays a role in stabilizing the compound's position in the binding site.

With regard to the hydroxyl group at the C3 position, this functionality establishes hydrogen bonds with Ser168 (**3a**), or with Asp178 (**4a**, **4c**, **4d**) helping to stabilize the ligand within SphK1's binding site.

Regarding the participation of the polar headgroups of these compounds in binding interactions, the dimethylamine group in **3a** adopts a more folded conformation relative to the main chain compared to that observed in SphK2, thus facilitating the hydrogen bonding involving OH-3 and the triazole ring mentioned above. Meanwhile, the guanidino group in **4a–d** forms a two-hydrogen-bond motif with the backbone carbonyl group of Leu268, reinforcing their binding to SphK1 in a similar way to that observed for SphK2. Compared to the Sphk2 binding motif, in Sphk1, the third hydrogen bond with the aspartate amino acid is lost. Thus, the guanidino group interaction could be a key factor in the potency of these compounds.

Lastly, the hydrophobic tail in the non-fluorinated derivative **3a** fits well within the hydrophobic toe of the binding site, adopting a different orientation to that of the trifluoromethylated lipophilic tail in **3b**. As the degree of fluorination increases in compounds **4c** and **4d** (see comparative figures in the ESI†), the tail becomes more rigid and fits well into the pocket.

Among the *N*,*N*-dimethyl amino series **3**, the fact that **3c** and **3d** are bad inhibitors may be related to the extended conformation of the *N*,*N*-dimethylamino moiety (in contrast to the folded conformation of the guanidino group), which extends the fatty tail deeper in the hydrophobic cavity at the toe of the binding site, leading to loss of surface contact for those analogues with exceedingly high bulk, going from **3a** to **3d**.

Conclusions

In this study a series of 1-deoxysphingosine analogues incorporating a 1,2,3-triazole ring, modifications in the amino group (*N*-methyl, *N*,*N*-dimethyl and guanidino), and differently fluorinated tails have been successfully synthesized as potential sphingosine kinase inhibitors. The *anti*-2,3-aminoalcohol segment in the target molecules was constructed through diastereoselective nucleophilic addition of an organoalkynylide to L-alaninal derivatives with excellent *anti* diastereoisomeric ratios from the *N*,*N*-dibenzylated compound.

The synthesized compounds exhibited dual inhibition of SphK1 and SphK2, with a general trend of higher selectivity towards SphK2. Among the different analogues, the guanidino compounds, particularly heptafluoro derivative **4a**, emerged as the most potent inhibitor (IC_{50} = 5.0 μM), displaying significant selectivity for SphK2 (SphK2/SphK1 selectivity ratio = 10.0). The study also revealed that increasing the degree of fluorination in the lipophilic tail did not always correlate with increased selectivity or potency, underscoring the complexity of the interactions within the SphK binding sites.

The homology model built for Sphk2 shows that differences in amino acid residues between SphK1 and SphK2 at key positions, such as Val340, Leu553, and Cys569 in SphK2 replacing Ile174, Met272, and Phe288 in SphK1, lead to structural

changes that affect the contact surface and orientation of key residues. These include Phe192 in SphK1, which protrudes, and Phe358 in SphK2, which buries into the J-channel. Additionally, Arg357 in SphK2 is more exposed than its homolog in SphK1, Arg191.

Docking studies provided valuable insights into the binding modes of the most potent inhibitors, mainly dependent on the polar head group. Thus, the guanidino derivatives showed distinct binding interactions, including hydrogen bonding with key residues such as Asp247 and Leu549 in SphK2 and Leu268 in SphK1. The orientation of the triazole ring, favoring π-stacking interactions with Phe358 in Sphk2, is also a critical factor influencing the optimal binding conformation of the molecules.

As a general trend, the presence of a terminal trifluoromethyl fragment at the hydrophobic tail resulted in detrimental activity within the same series of compounds, whereas compounds with a terminal heptafluoropropyl fragment showed an enhancement of SphK binding probably by rigidifying the end of the lipophilic tail, positioning it to perfectly fit the toe of the binding site.

Overall, this study advances the understanding of sphingosine kinase inhibition, as well as the knowledge of the differential topology of the active pockets of SphK1 and SphK2 and lays additional foundations for the development of novel 1-deoxysphingosine analogues targeting this pathway.

The results presented here suggest opportunities for further studies, particularly exploring modifications to chain length and functionalities, and in this sense, prospective studies are underway. For the time being, however, these results point to the potential use of terminal heptafluoropropyl groups and polar guanidinium heads as structural motifs in designing 1-deoxysphingosine analogues towards improving SphK2 inhibition.

Author contributions

Adrià Cardona: formal analysis, investigation, and methodology. Varbina Ivanova: formal analysis, investigation, and methodology. Raúl Beltrán-Debón: investigation. Xavier Barril: methodology. Sergio Castillón: supervision and funding acquisition. Yolanda Díaz: investigation, methodology, supervision, writing – original draft, and writing – review & editing. M. Isabel Matheu: investigation, methodology, supervision, writing – original draft, writing – review & editing, visualization, project administration, and funding acquisition.

Data availability

The data supporting this article have been included as part of the ESI.†

Conflicts of interest

There are no conflicts to declare.

Acknowledgements

We acknowledge Grant PID2021-125923OB-I00 funded by Ministerio de Ciencia e Innovación, Spain (MCIN) and Agencia Estatal de Investigación, Spain (AEI), MCIN/AEI/10.13039/501100011033, and by "European Regional Development Fund (ERDF), A way of making Europe". A.C. acknowledges Universitat Rovira i Virgili, Spain, for a predoctoral fellowship (E-43-2015-0002625). V.I. acknowledges the EU Horizon 2020 MSCA Program for grant agreement 956314 (ALLODD).

References

1 T. A. Taha, Y. A. Hannun and L. M. Obeid, *J. Biochem. Mol. Biol.*, 2006, **39**, 113.
2 (*a*) M. M. Young, M. Kester and H.-G. Wang, *J. Lipid Res.*, 2013, **54**, 5; (*b*) M. Maceyka, K. B. Harikumar, S. Milstien and S. Spiegel, *Trends Cell Biol.*, 2012, **22**, 50; (*c*) S. Ponnusamy, M. Meyers-Needham, C. E. Senkal, S. A. Saddoughi, D. Sentelle, S. P. Selvam, A. Salas and B. Ogretmen, *Future Oncol.*, 2010, **6**, 1603; (*d*) W. Jiang and B. Ogretmen, *Biochim. Biophys. Acta, Mol. Cell Biol. Lipids*, 2014, **1841**, 783.
3 (*a*) N. C. Hait, C. A. Oskeritzian, S. W. Paugh, S. Milstien and S. Spiegel, *Biochim. Biophys. Acta*, 2006, **1758**, 2016; (*b*) S. M. Pitson, *Trends Biochem. Sci.*, 2011, **36**, 97.
4 D. Hatoum, N. Haddadi, Y. Lin, N. T. Nassif and E. M. McGowan, *Oncotarget*, 2017, **8**, 36898.
5 (*a*) K. Shirai, T. Kaneshiro, M. Wada, H. Furuya, J. Bielawski, Y. A. Hannun, L. M. Obeid, B. Ogretmen and T. Kawamori, *Cancer Prev. Res.*, 2011, **4**, 454; (*b*) W. Li, C. P. Yu, J. T. Xia, L. Zhang, G. X. Weng, H.-Q. Zheng, Q. L. Kong, L.-J. Hu, M.-S. Zeng, Y.-X. Zeng, M. Li, J. Li and L. B. Song, *Clin. Cancer Res.*, 2009, **15**, 1393; (*c*) K. R. Johnson, K. Y. Johnson, H. G. Crellin, B. Ogretmen, A. M. Boylan, R. A. Harley and L. M. Obeid, *Histochem. Cytochem.*, 2005, **53**, 1159; (*d*) R. Erez-Roman, R. Pienik and A. H. Futerman, *Biochem. Biophys. Res. Commun.*, 2010, **391**, 219; (*e*) E. Ruckhäberle, A. Rody, K. Engels, R. Gaetje, G. von Minckwitz, S. Schiffmann, S. Grösch, G. Geisslinger, U. Holtrich, T. Karn and M. Kaufmann, *Breast Cancer Res. Treat.*, 2008, **112**, 41; (*f*) T. Kawamori, T. Kaneshiro, M. Okumura, S. Maalouf, A. Uflacker, J. Bielawski, Y. A. Hannun and L. M. Obeid, *FASEB J.*, 2009, **23**, 405.
6 (*a*) C. T. Wallington-Beddoe, J. A. Powell, D. Tong, S. M. Pitson, K. F. Bradstock and L. J. Bendall, *Cancer Res.*, 2014, **74**, 2803; (*b*) S. W. Paugh, B. S. Paugh, M. Rahmani, D. Kapitonov, J. A. Almenara, T. Kordula, S. Milstien, J. K. Adams, R. E. Zipkin, S. Grant and S. A. Spiegel, *Blood*, 2008, **112**, 1382; (*c*) E. Bonhoure, A. Lauret, D. J. Barnes, C. Martin, B. Malavaud, T. Kohama, J. V. Melo and O. Cuvillier, *Leukemia*, 2008, **22**, 971.
7 (*a*) W. Li, Z. Tian, H. Qin, N. Li, X. Zhou, J. Li, B. Ni and Z. Ruan, *Biochem. Biophys. Res. Commun.*, 2015, **460**, 341; (*b*) H. Xiong, J. Wang, H. Guan, J. Wu, R. Xu, M. Wang,

X. Rong, K. Huang, J. Huang, Q. Liao, Y. Fu and J. Yuan, *Oncol. Rep.*, 2014, **32**, 1369.

8 L. Hasanifard, R. Sheervalilou, M. Majidinia and B. Yousefi, *J. Cell. Physiol.*, 2019, **234**, 8162.

9 (*a*) E. Magli, A. Corvino, F. Fiorino, F. Frecentese, E. Perissutti, I. Saccone, V. Santagada, G. Caliendo and B. Severino, *Curr. Pharm. Des.*, 2019, **25**, 956; (*b*) V. K. R. Tangadanchu, H. Jiang, Y. Yu, T. J. A. Graham, H. Liu, B. E. Rogers, R. Gropler, J. Perlmutter and Z. Tu, *Eur. J. Med. Chem.*, 2020, **206**, 112713; (*c*) A. Corvino, R. Rosa, G. M. Incisivo, F. Fiorino, F. Frecentese, E. Magli, E. Perissutti, I. Saccone, V. Santagada, G. Cirino, M. A. Riemma, P. A. Temussi, P. Ciciola, R. Bianco, G. Caliendo, F. Roviezzo and B. Severino, *Int. J. Mol. Sci.*, 2017, **18**, 2332; (*d*) J. Cho, Y. M. Lee, D. Kim and S. Kim, *J. Org. Chem.*, 2009, **74**, 3900; (*e*) J.-W. Kim, Y.-W. Kim, Y. Inagaki, Y.-A. Hwang, S. Mitsutake, Y.-W. Ryu, W. K. Lee, H.-J. Ha, C.-S. Parka and Y. Igarashi, *Bioorg. Med. Chem.*, 2005, **13**, 3475; (*f*) K. Kim, Y.-L. Kim, S. J. Sacket, H.-L. Kim, M. Han, D. S. Park, B. K. Lee, W. K. Lee, H.-J. Ha and D.-S. Im, *J. Pharm. Pharmacol.*, 2007, **59**, 1035.

10 M. A. Lone, T. Santos, I. Alecu, L. C. Silva and T. Hornemann, *Biochim. Biophys. Acta, Mol. Cell Biol. Lipids*, 2019, **1864**, 512.

11 R. Cuadros, E. Montejo de Garcini, F. Wandosell, G. Faircloth, J. M. Fernández-Sousa and J. Avila, *Cancer Lett.*, 2000, **152**, 23.

12 (*a*) A. Aiello, E. Fattorusso, A. Giordano, M. Menna, C. Navarrete and E. Muñoz, *Bioorg. Med. Chem.*, 2007, **15**, 2920; (*b*) A. Aiello, E. Fattorusso, A. Giordano, M. Menna, C. Navarrete and E. Muñoz, *Tetrahedron*, 2009, **65**, 4384.

13 E. A. Jares-Erijman, C. P. Bapat, A. Lithgow-Bertelloni, K. L. Rinehart and R. Sakai, *J. Org. Chem.*, 1993, **58**, 5732.

14 C. Jimenez and P. Crews, *J. Nat. Prod.*, 1990, **53**, 978.

15 H. Symolon, A. Bushnev, Q. Peng, H. Ramaraju, S. G. Mays, J. C. Allegood, S. T. Pruett, M. C. Sullards, D. L. Dillehay, D. C. Liotta and A. H. Merrill Jr., *Mol. Cancer Ther.*, 2011, **10**, 648.

16 H. U. Humpf, E.-M. Schmelz, F. I. Meredith, H. Vesper, T. R. Vales, E. Wang, D. S. Menaldino, D. C. Liotta and A. H. Merrill Jr., *J. Biol. Chem.*, 1998, **273**, 19060.

17 D. S. Menaldino, A. Bushnev, A. Sun, D. C. Liotta, H. Symolon, K. Desai, D. L. Dillehay, Q. Peng, E. Wang, J. Allegood, S. Trotman-Pruett, M. C. Sullards and A. H. Merrill Jr., *Pharmacol. Res.*, 2003, **47**, 373.

18 (*a*) J. Guasch, I. Giménez-Nueno, I. Funes-Ardoiz, M. Bernús, M. I. Matheu, F. Maseras, S. Castillón and Y. Díaz, *Chem. – Eur. J.*, 2018, **24**, 4635; (*b*) J. Llaveria, A. Beltrán, W. M. C. Sameera, A. Locati, M. M. Díaz-Requejo, M. I. Matheu, S. Castillón, F. Maseras and P. J. Pérez, *J. Am. Chem. Soc.*, 2014, **136**, 5342; (*c*) J. Guasch, Y. Díaz, M. I. Matheu and S. Castillón, *Chem. Commun.*, 2014, **50**, 7344; (*d*) J. A. Morales-Serna, J. Llaveria, Y. Díaz, M. I. Matheu and S. Castillón, *Curr. Org. Chem.*, 2010, **14**, 2483; (*e*) J. Llaveria, A. Beltrán, M. M. Díaz-Requejo, M. I. Matheu, S. Castillón and P. J. Pérez, *Angew. Chem., Int. Ed.*, 2010, **49**, 7092; (*f*) J. A. Morales-Serna, Y. Díaz, M. I. Matheu and S. Castillón, *Synthesis*, 2009, **5**, 710; (*g*) J. Llaveria, Y. Díaz, M. I. Matheu and S. Castillón, *Org. Lett.*, 2009, **11**, 205; (*h*) J. A. Morales-Serna, J. Llaveria, Y. Díaz, M. I. Matheu and S. Castillón, *Org. Biomol. Chem.*, 2008, **6**, 4502; (*i*) P. Rivero, V. Ivanova, X. Barril, M. Casampere, J. Casas, G. Fabriàs, Y. Díaz and M. I. Matheu, *Bioorg. Chem.*, 2024, **145**, 107233.

19 (*a*) M. Escudero-Casao, A. Cardona, R. Beltrán-Debón, Y. Díaz, M. I. Matheu and S. Castillón, *Org. Biomol. Chem.*, 2018, **16**, 7230; (*b*) M. Corro-Morón, A. Granell, V. Ivanova, E. Domingo, R. Beltrán-Debón, X. Barril, M.-J. Sanz, M. I. Matheu, S. Castillón and Y. Díaz, *Bioorg. Chem.*, 2022, **121**, 105668.

20 The dipole moment for 1,4-disubstituted-1,2,3-triazole is 4.18 D. See: J.-L. M. Abboud, C. Foces-Foces, R. Notario, R. E. Trifonov, A. P. Volovodenko, V. A. Ostrovskii, I. Alkorta and J. Elguero, *Eur. J. Org. Chem.*, 2001, 3013.

21 (*a*) M. A. Miller and E. M. Sletten, *ChemBioChem*, 2020, **21**, 3451; (*b*) M. Bassetto, S. Ferla and F. Pertusati, *Future Med. Chem.*, 2015, **7**, 527.

22 In relation to the fluorine effect on compounds interacting with hydrophobic fragments of proteins, see: L. Liu, N. Jalili, A. Baergen, S. Ng, J. Bailey, R. Derda and J. S. Klassen, *J. Am. Soc. Mass Spectrom.*, 2014, **25**, 751.

23 Incorporating rigid elements into flexible ligands to enhance protein–ligand binding affinity directly influences the entropic component of Gibbs free energy. See: (*a*) M. Schauperl, M. Podewitz, B. J. Waldner and K. R. Liedl, *J. Chem. Theory Comput.*, 2016, **12**, 4600; (*b*) G. Klebe, F. Dullweber and H.-J. Böhm, Thermodynamic models of drug-receptor interactions: a general introduction, in *Drug-Receptor Thermodynamics: Introduction and Applications*, John Wiley & Sons, Chichester, UK, 2001, 83–104; (*c*) I. D. Kuntz, K. Chen, K. A. Sharp and P. A. Kollman, *Proc. Natl. Acad. Sci. U. S. A.*, 1999, **96**, 9997.

24 M. T. Reetz, M. W. Drewes and A. Schmitz, *Angew. Chem.*, 1987, **99**, 1186.

25 (*a*) G. Silveira-Dorta, O. J. Donadel, V. S. Martín and J. M. Padrón, *J. Org. Chem.*, 2014, **79**, 6775; (*b*) G. Silveira-Dorta, I. J. Sousa, M. X. Fernandes, V. S. Martín and J. M. Padrón, *Eur. J. Med. Chem.*, 2015, **96**, 308.

26 R. A. da Silva, I. H. S. Estevam and L. W. Bieber, *Tetrahedron Lett.*, 2007, **48**, 7680.

27 M. A. Ayoub, J. Trebaux, J. Vallaghe, F. Charrier-Savournin, K. Al-Hosaini, A. Gonzalez Moya, J.-P. Pin, K. D. G. Pfleger and E. Trinquet, *Front. Endocrinol.*, 2014, **5**, 1.

28 (*a*) T. A. Klink, K. M. Kleman-Leyer, A. Kopp, T. A. Westermeyer and R. G. Lowery, *J. Biomol. Screening*, 2008, **13**, 476; (*b*) Adapta Universal Kinase Assay User Guide. Protocol part PV5099. Rev. 14 February 2008. Invitrogen.

29 D. Soler, Y. Westermaier and R. Soliva, *J. Comput. Aided Mol. Des.*, 2019, **33**, 613.

30 D. R. Adams, S. Tawati, G. Berretta, P. Lopez Rivas, J. Baiget, Z. Jiang, A. Alsfouk, S. P. Mackay, N. J. Pyne and S. Pyne, *J. Med. Chem.*, 2019, **62**, 3658.